Hindawi Publishing Corporation
Advances in Tribology
Volume 2008, Article ID 871952, 10 pages
doi:10.1155/2008/871952

Research Article

Performance of an Orifice Compensated Two-Lobe Hole-Entry Hybrid Journal Bearing

J. Sharana Basavaraja, Satish C. Sharma, and S. C. Jain

Department of Mechanical and Industrial Engineering, Indian Institute of Technology, Roorkee 247 667, India

Correspondence should be addressed to J. Sharana Basavaraja, khinaresh@gmail.com

Received 4 October 2007; Revised 24 December 2007; Accepted 6 February 2008

Recommended by Abdallah Elsharkawy

The work presented in this paper aims to study the performance of a two-lobe hole-entry hybrid journal bearing system compensated by orifice restrictors. The Reynolds equation governing the flow of lubricant in the clearance space between the journal and bearing together with the equation of flow through an orifice restrictor has been solved using FEM and Galerkin's method. The bearing performance characteristics results have been simulated for an orifice compensated nonrecessed two-lobe hole-entry hybrid journal bearing symmetric configuration for the various values of offset factor (δ), restrictor design parameter ($\overline{C}_{S2}$), and the value of external load ($\overline{W}_0$). Further, a comparative study of the performance of a two-lobe hole-entry hybrid journal bearing system with a circular hole-entry symmetric hybrid journal bearing system has also been carried out so that a designer has a better flexibility in choosing a suitable bearing configuration. The simulated numerical results indicate that for the two-lobe symmetric hole-entry hybrid journal bearing system with an offset factor (δ) greater than one provides 30 to 50 percent larger values of direct stiffness and direct damping coefficients as compared to a circular symmetric hole-entry hybrid journal bearing system.

1. INTRODUCTION

Hybrid journal bearings are extensively used in machine tools under conditions of heavy loads and higher speeds. The stability and unsteady behavior of the hybrid journal bearings is greatly influenced by bearing geometry, and accordingly various designs have been used by designers to achieve the desired objective. To ensure better dynamic stability than a circular plain journal bearing, multilobe journal bearings are used. Multilobe hydrodynamic journal bearings have been investigated for their antiwhril characteristics by many researchers [1–5]. Pinkus [1] studied the performance of an elliptical journal bearing in terms of steady-state load carrying capacity and power loss using the FDM. Malik [2] theoretically studied an elliptical hydrodynamic journal bearing and compared its performance over a wide range of load conditions and provided the comprehensive design data including the static and dynamic characteristics for the two-lobed journal bearing for different aspect ratios. The study dealing with the effects of surface ellipticity on the dynamically loaded cylindrical bearing was carried out by Goenka and Booker [3] for an optimum bearing shape on the basis of maximizing the minimum film thickness. The notable observation about these studies is that they are all concerned with hydrodynamic journal bearing systems. Few studies dealing with the noncircular multirecess hydrostatic/hybrid journal bearing systems have also been reported in literature recently [6–8]. Ghosh and Satish [7], using a small amplitude perturbation analysis, determined the rotordynamic coefficients of a multilobe hybrid journal bearing system having large recesses. They extended their work further [8] to study the stability of a rigid rotor supported on a multilobe hybrid journal bearing system with short sills following a linear vibration theory for small amplitude oscillations of the journal center about its steady-state position. It was observed that a multilobe recessed hybrid journal bearing system with an offset factor more than one exhibits better dynamic performance than the circular hybrid journal bearings. The recessed journal bearings are unable to generate a substantial hydrodynamic action because recess constitutes a large bearing area, thus leaving very less area for lands. Thus, recessed bearings when

operating in hybrid mode at higher speeds are not suitable for heavily loaded applications. Hence, nonrecessed journal bearings, that is, hole-entry hybrid journal bearings were developed to gain the advantage of available large land area to generate substantial hydrodynamic action. Such bearings give better performance than the recessed bearings along with the ease of manufacture and reduced cost of machining [9–12].

Recent developments towards the use of hybrid bearings in high-speed turbopumps and advanced machine tools have further necessitated to focus research activities in the area of hybrid bearings. Most of the available nonrecessed hydrostatic/hybrid bearing studies are generally confined to circular bearings [13–15]. However, a thorough review of literature reveals that the performance of nonrecessed multilobe hole-entry hybrid journal bearing has not yet been investigated. Therefore, a study of a nonrecessed multilobe hole-entry hybrid journal bearing is planned to bridge the gap in literature. In this paper, nonrecessed orifice compensated two-lobe hole-entry hybrid journal bearing is investigated for its static and dynamic characteristics. The performance characteristics of two-lobe hole-entry hybrid journal bearing have been compared with that of a circular hole-entry orifice compensated hybrid journal bearing for the same bearing operating and geometric parameters. Results are presented for various values of offset factor (δ), restrictor design parameter ($\overline{C}_{S2}$), and for the value of external load for symmetric hole configuration. The computed results presented in this work are expected to be quite useful to the bearing designers as well as for the academic community.

2. ANALYSIS

The Reynolds equation governing the laminar flow of an incompressible lubricant in the clearance space of journal and bearing in nondimensional form is expressed as [16, 17]

$$\frac{\partial}{\partial\alpha}\left(\frac{\overline{h}^3}{6}\frac{\partial\overline{p}}{\partial\alpha}\right)+\frac{\partial}{\partial\beta}\left(\frac{\overline{h}^3}{6}\frac{\partial\overline{p}}{\partial\beta}\right)=\Omega\frac{\partial\overline{h}}{\partial\alpha}+2\frac{\partial\overline{h}}{\partial\overline{t}}. \tag{1}$$

3. FLUID FILM THICKNESS

The geometry of the symmetric hole-entry circular as well as multilobe hybrid journal bearing has been shown schematically in Figures 1(a) and 1(b). The expression for nondimensional fluid film thickness for a multilobe rigid journal bearing with reference to fixed coordinate axis is given as [6]

$$\overline{h}=\frac{1}{\delta}-(\overline{X}_j+\overline{x}-\overline{X}_L^i)\cos\ \alpha-(\overline{Z}_j+\overline{z}-\overline{Z}_L^i)\sin\alpha, \tag{2}$$

where $\overline{X}_j$ and $\overline{Z}_j$ are the equilibrium coordinates of the journal center, and $\overline{x}$ and $\overline{z}$ are time dependent perturbation coordinates of the journal center measured from their equilibrium position ($\overline{x},\overline{z}=0$ for steady case). $\overline{X}_L^i$ and $\overline{Z}_L^i$ are the lobe center coordinates of ith lobe.

4. RESTRICTOR FLOW EQUATION

The flow rate of the lubricant through the orifice restrictor is defined as [17]

$$\overline{Q}_R=\overline{C}_{S2}(1-\overline{p}_c)^{1/2}, \tag{3}$$

where the term $\overline{p}_c$ represents the pressure at the hole.

5. FINITE ELEMENT FORMULATION

The lubricant flow field in the clearance space of a circular bearing has been discretized into four-noded isoparametric elements and using the Lagrangian interpolation function, the pressure at a point in the element is bilinearly distributed and expressed approximately as [18]

$$\overline{p}=\sum_{j=1}^{4}N_j\overline{p}_j, \tag{4}$$

where N_j is elemental shape function, and using the approximate value of $\overline{p}$ (1) can be expressed as

$$\begin{aligned}&\frac{\partial}{\partial\alpha}\left[\frac{\overline{h}^3}{6}\frac{\partial}{\partial\alpha}\left(\sum_{j=1}^{4}N_j\overline{p}_j\right)\right]+\frac{\partial}{\partial\beta}\left[\frac{\overline{h}^3}{6}\frac{\partial}{\partial\beta}\left(\sum_{j=1}^{4}N_j\overline{p}_j\right)\right]\\&\quad-\Omega\frac{\partial\overline{h}}{\partial\alpha}-2\frac{\partial\overline{h}}{\partial\overline{t}}=R^e,\end{aligned} \tag{5}$$

where R^e is known as residue. The element equations are obtained by applying Galerkin's technique. As per this technique, minimization of residue is obtained by orthogonalizing the residue with interpolation functions, that is,

$$\iint_{\Omega^e}N_iR^e\,d\alpha\,d\beta=0. \tag{6}$$

By integrating the second-order term by parts to obtain C^0 continuity and differentiating (4) with respect to $\overline{t}$, the resulting equation for a typical element is obtained in matrix form as follows:

$$\begin{aligned}&[\overline{F}]_{n\times n}\{\overline{p}\}_{n\times1}\\&\quad=\{\overline{Q}\}_{n\times1}+\Omega\{\overline{R}_H\}_{n\times1}+\dot{\overline{x}}_j\{\overline{R}_{x_j}\}_{n\times1}+\dot{\overline{z}}_j\{\overline{R}_{z_j}\}_{n\times1},\end{aligned} \tag{7}$$

where n = total number of nodes in lubricant flow field.

After modification for continuity of flow between bearing and restrictor and incorporating appropriate boundary condition, the system (7) is solved for nodal pressure and nodal flows.

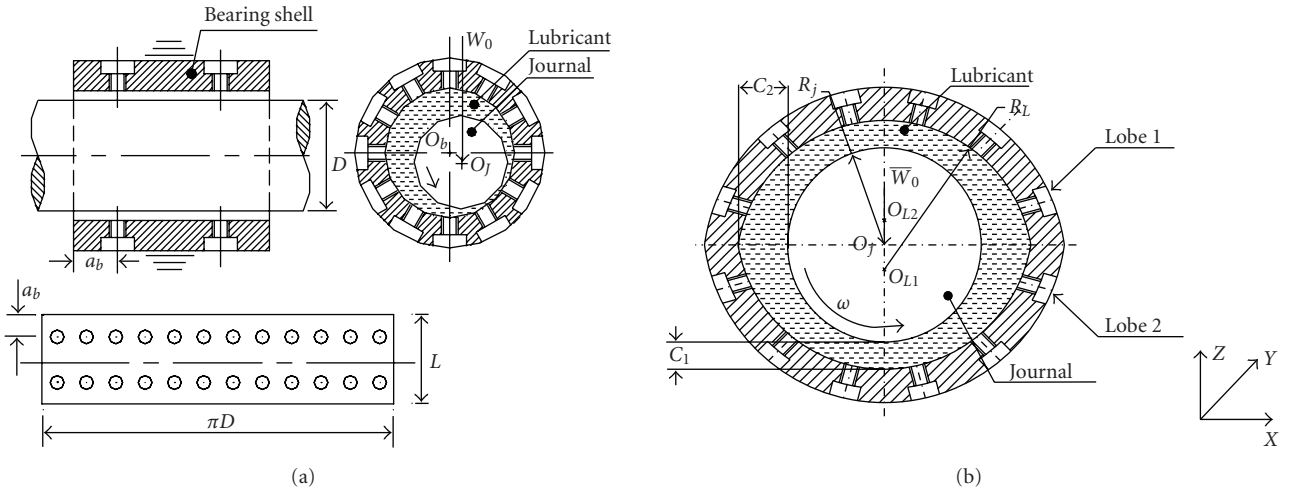

Figure 1: (a) Hole-entry type journal bearing system (symmetric configuration). (b) Two-lobe hole-entry type journal bearing system (symmetric configuration).

For an eth element, the elements of the above matrices are defined as follows:

$$\overline{F}_{ij}^{e} = \iint_{A^e} \overline{h}^3 \overline{F}_2 \left[\frac{\partial N_i}{\partial \alpha}\frac{\partial N_j}{\partial \alpha} + \frac{\partial N_i}{\partial \beta}\frac{\partial N_j}{\partial \beta} \right] d\alpha\, d\beta, \tag{7a}$$

$$\overline{Q}_i^e = \int_{\Gamma^e} \left\{ \left(\overline{h}^3 \overline{F}_2 \frac{\partial \overline{p}}{\partial \alpha} - \Omega \left(1 - \frac{\overline{F}_1}{\overline{F}_0} \right) \overline{h} \right) l + \left(\overline{h}^3 \overline{F}_2 \frac{\partial \overline{p}}{\partial \beta} \right) m \right\} N_i d\,\overline{\Gamma}^{e}, \tag{7b}$$

$$\overline{R}_{H_i}^{e} = \iint_{A^e} \left\{ \left(1 - \frac{\overline{F}_1}{\overline{F}_0} \right) \overline{h} \right\} \frac{\partial N_i}{\partial \alpha} d\alpha\, d\beta, \tag{7c}$$

$$\overline{R}_{X_{Ji}}^{e} = \iint_{A^e} N_i \cos\alpha \; d\alpha\, d\beta, \tag{7d}$$

$$\overline{R}_{Z_{Ji}}^{e} = \iint_{A^e} N_i \sin\alpha \; d\alpha\, d\beta, \tag{7e}$$

where l and m are the directions cosines and $i, j = 1, 2, \ldots, n_l^e$ (number of nodes per element).

6. BOUNDARY CONDITIONS

The boundary conditions for the lubricant flow field are as follows.

(1) Nodes situated on the external boundary of the bearing have zero pressure,

$$\overline{p}|_{\beta = \mp 1.0} = 0.0. \tag{8}$$

(2) The nodes situated on a hole have equal pressure.
(3) Flow of lubricant through the restrictor is equal to the bearing input flow.
(4) The nodal flows are zero at internal nodes except those situated on holes.

7. SOLUTION PROCEDURE

The study of an orifice compensated multilobe hole-entry hybrid journal bearing system needs an iterative solution scheme to establish solutions of the flow field system (5) with the restrictor flow (3) as constraint with boundary conditions. Assuming constant viscosity and the steady-state case ($\dot{\overline{X}}_j, \dot{\overline{Z}}_j = 0$), the lubricant flow field system (5), after adjustment for flow through orifice restrictor (3) and modification for boundary conditions, is solved for a specified journal center position $(\overline{X}_j, \overline{Z}_j)$ using Gauss elimination technique. If the solution is to be obtained for a specified vertical external load, one additional iterative loop is needed to establish the equilibrium journal center position using the following equations:

$$\overline{F}_x = 0, \qquad \overline{F}_z - \overline{W}_0 = 0. \tag{9}$$

The fluid-film reaction terms $\overline{F}_x$ and $\overline{F}_z$ in (9) are expanded by Taylor series about the ith journal center position, and the increments $(\Delta\overline{X}_j^i, \Delta\overline{Z}_j^i)$ on the journal coordinates are obtained. Iterations are continued until the following convergence criterion is not satisfied:

$$\left[\frac{\left(\left(\Delta\overline{X}_j^i \right)^2 + \left(\Delta\overline{Z}_j^i \right)^2 \right)^{1/2}}{\left(\left(\overline{X}_j^i \right)^2 + \left(\overline{Z}_j^i \right)^2 \right)^{1/2}} \right] \times 100 < 0.001, \tag{10}$$

where $\overline{X}_j^i$, $\overline{Z}_j^i$ are the coordinates of the ith journal center position. The overall iterative solution scheme is presented in Figure 2.

8. FLUID FILM STIFFNESS AND DAMPING COEFFICIENTS

Fluid-film stiffness and damping coefficients are computed using the expressions given below.

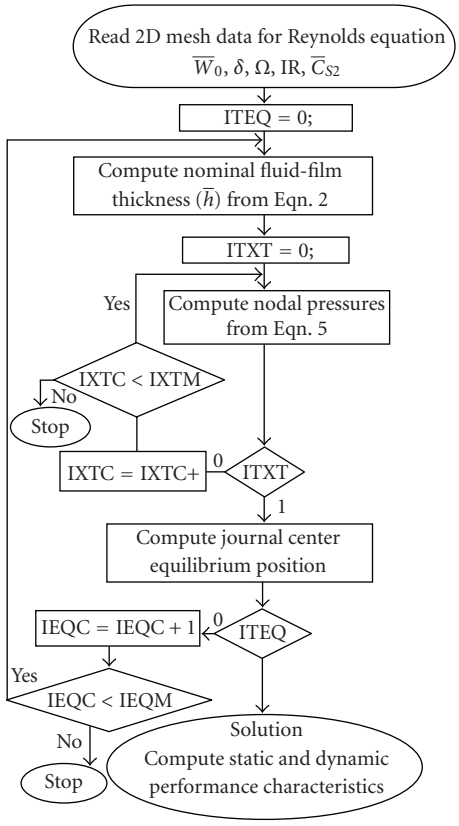

IEQC: Iteration counter for journal center equilibrium
IXTC: Iteration counter for extent of fluid film
IEQM: Maximum number of iteration for journal center equilbrium
IXTM: Maximum number of iteration for extent of fluid film
IR: Code for type of restrictor

Figure 2: Overall iterative scheme.

Fluid-film stiffness coefficients:

$$\overline{S}_{ij} = -\frac{\partial \overline{F}_i}{\partial \overline{q}_J}, \quad (i = x, z), \tag{11}$$

where

i = direction of force or moment.

$\overline{q}_J$ = direction of journal center displacement ($\overline{q}_J = \overline{X}_J, \overline{Z}_J$).

Fluid-film damping coefficients:

$$\overline{C}_{ij} = -\frac{\partial \overline{F}_i}{\partial \dot{\overline{q}}_J}, \quad (i = x, z), \tag{12}$$

here, $\dot{\overline{q}}_J$ represents the velocity component of journal center ($\dot{\overline{q}}_J = \dot{\overline{X}}_J, \dot{\overline{Z}}_J$).

9. RESULTS AND DISCUSSION

The performance characteristics for circular and two-lobe symmetric hole-entry hybrid journal bearing have been computed using the solution scheme as discussed earlier. The results have been computed for various values of offset factor (δ) and restrictor design parameter ($\overline{C}_{S2}$). The chosen values of bearing operating parameter are most generally used values as given in Table 1.

Table 1: Bearing operating and geometric parameters.

Bearing aspect ratio (λ)	1
Land width ratio ($\overline{a}_b$)	0.25
Restrictor design parameter ($\overline{C}_{S2}$)	0.02–0.1
Offset factor (δ)	0.5, 0.75, 1.0, 1.25, 1.5
External load ($\overline{W}_0$)	1.25
Number of holes per row	12
Number of rows	2
Concentric pressure ratio (β^*)	0.5
Type of restrictor	orifice

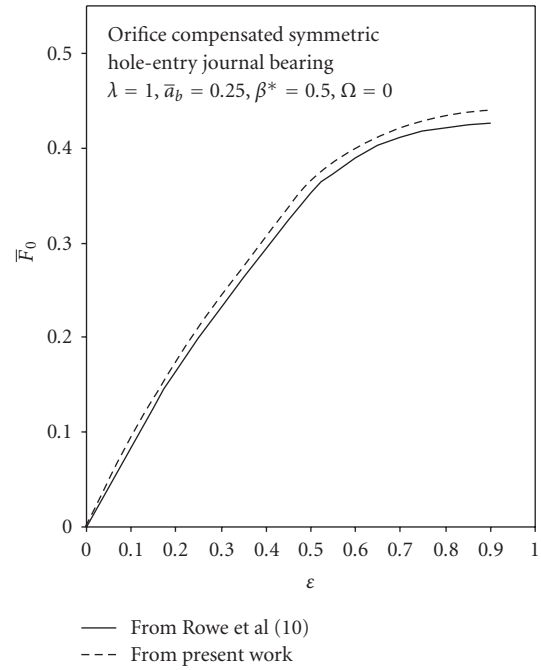

Figure 3: Variation of external load carrying capacity ($\overline{F}_0$) with eccentricity (ε).

In order to check the validity of the computed results obtained from the developed program, the computed results have been compared with those already available in the literature. To the best of author's knowledge, no results are available in the literature for the performance characteristics of nonrecessed multilobe hole-entry hybrid journal bearing. Hence, to validate the results, first the values of fluid film reaction ($\overline{F}_0$) for orifice compensated hole-entry hydrostatic journal bearing are computed and compared with that of Rowe et al. [10]. The results compare well for wide range of eccentricity ratio (ε) as shown in Figure (3). Further, using Reynolds cavitation boundary condition, the performance characteristics of two-lobe hydrodynamic journal bearing are compared with the data of Lund and Thomsen [19]. The results match very well as shown in Table 2.

Table 2: Comparison of performance characteristics of two-lobe hydrodynamic journal bearing, $L/D = 1$, $\Omega = 1$, $\delta = 0.5$. $\overline{W}_0 = 5.0$.

Characteristics	Present	Ref. [19]
ε	0.3426	0.340
ϕ	80.997	82.100
$\overline{S}_{xx}/\overline{W}_0$	1.203	1.110
$\overline{S}_{xz}/\overline{W}_0$	1.812	1.700
$\overline{S}_{zx}/\overline{W}_0$	−3.5004	−3.610
$\overline{S}_{zz}/\overline{W}_0$	5.1544	5.130
$\overline{C}_{xx}/\overline{W}_0$	2.801	2.620
$-(\overline{C}_{xz} = \overline{C}_{zx})/\overline{W}_0$	0.2568	0.238
$\overline{C}_{zz}/\overline{W}_0$	9.3348	9.430

The static and dynamic performance characteristics which include maximum pressure ($\overline{p}$), minimum fluid film thickness ($\overline{h}_{\min}$), bearing flow ($\overline{Q}$), stiffness coefficients ($\overline{S}_{ij}$), damping coefficients ($\overline{C}_{ij}$), and threshold speed ($\overline{\omega}_{\text{th}}$) have been presented for various values of offset factors (δ), restrictor design parameter ($\overline{C}_{S2}$), and external load ($\overline{W}_0$). The results are presented through Figures (4–14) and discussed in the following paragraph.

Figure 4 shows the variation of maximum pressure ($\overline{p}$). It has been observed that the value of maximum pressure ($\overline{p}$) for a specified external load increases with restrictor design parameter ($\overline{C}_{S2}$). From the graph, it may be observed for the given value of external load ($\overline{W}_0$) and the restrictor design parameter ($\overline{C}_{S2}$) that the value of maximum pressure is higher for two-lobe hole-entry hybrid journal bearing. It is also observed that the value of maximum pressure ($\overline{p}$) increases in case of two-lobe hole-entry hybrid journal bearing with offset factor (δ) more than one compared to circular hole-entry hybrid journal bearing. The decrease in the value of fluid film thickness ($\overline{h}$) owing to the change of geometry of the bearing is responsible for the increase in the value of maximum pressure ($\overline{p}$).

Figure 5 shows the variation of minimum fluid-film thickness ($\overline{h}_{\min}$). It is observed that the value of minimum fluid film thickness ($\overline{h}_{\min}$) for a specified external load reduces with an increase in restrictor design parameter ($\overline{C}_{S2}$) for all the cases of offset factor (δ) except for the case of offset factor $\delta = 0.5$. At a constant external load, the two-lobe hole-entry hybrid journal bearing with offset factor (δ) more than one operates at higher eccentricities compared to circular hole-entry hybrid journal bearing. Also Figure 5 indicates that the two-lobe hole-entry hybrid journal bearing with offset factor $\delta = 0.75$ operates with higher value of minimum fluid film thickness ($\overline{h}_{\min}$) compared to other cases of offset factor (δ). The increase or decrease in the value of minimum fluid film thickness ($\overline{h}_{\min}$) has been found of the order of 0.5 < .75 >1.0 >1.25 >1.3. The maximum value of minimum fluid film thickness ($\overline{h}_{\min}$) is not exactly for $\delta = 1.0$, but rather it is observed to be at the values between $\delta = 0.75$ and $\delta = 0.9$. Similar tend has been reported by Goenka and Booker [3]. This trend may be attributed due to the clearance change in the bearing for the values of offset factor (δ). It may be observed that a desired value of $\overline{h}_{\min}$ may be obtained in a

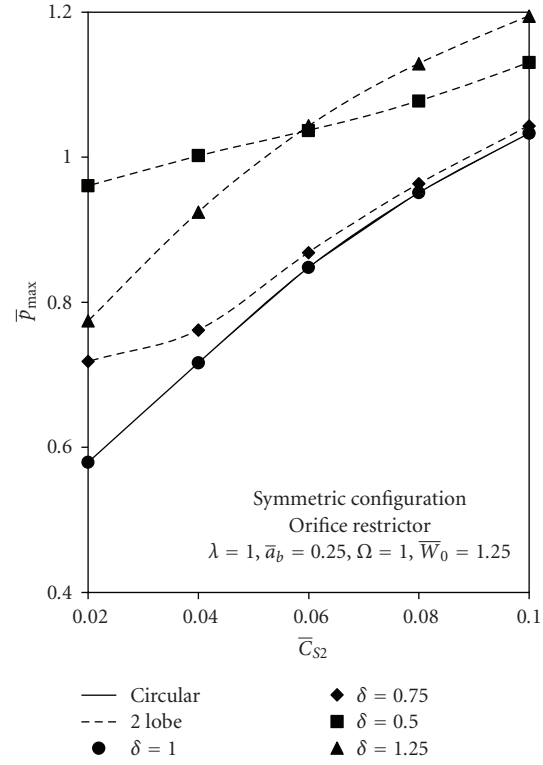

Figure 4: Variation of maximum pressure ($\overline{p}$).

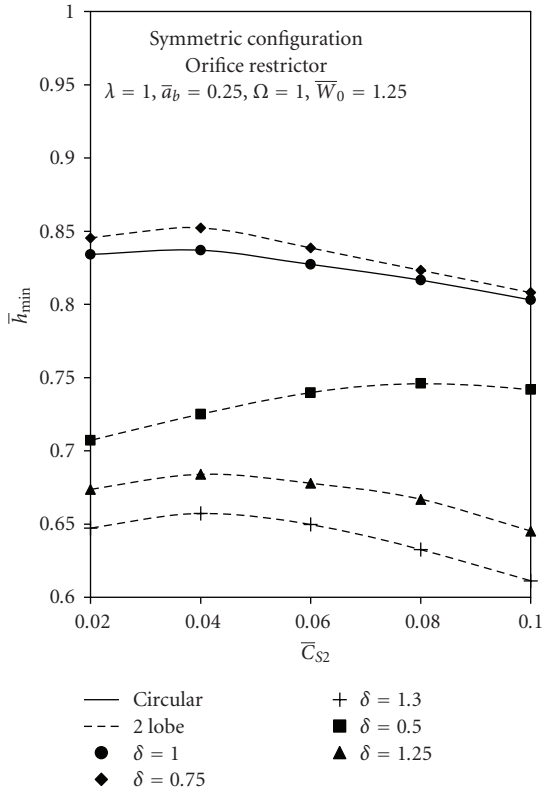

Figure 5: Variation of fluid film thickness ($\overline{h}$).

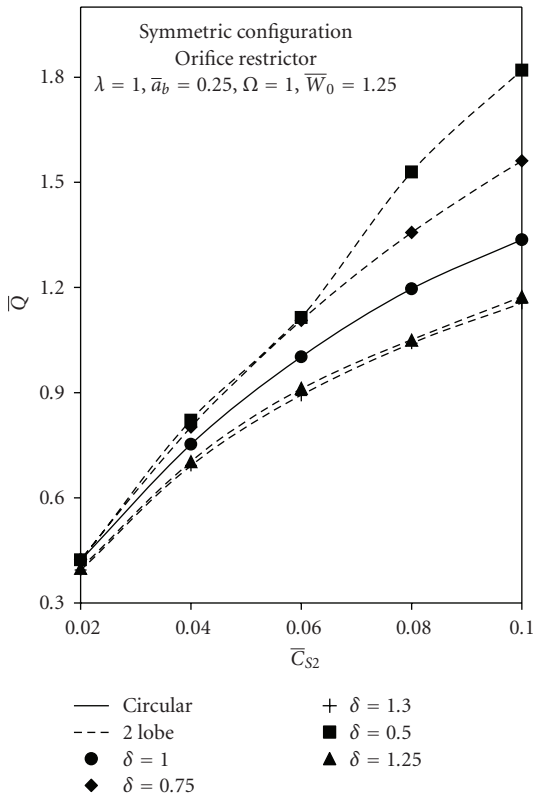

Figure 6: Variation of bearing flow ($\overline{Q}$).

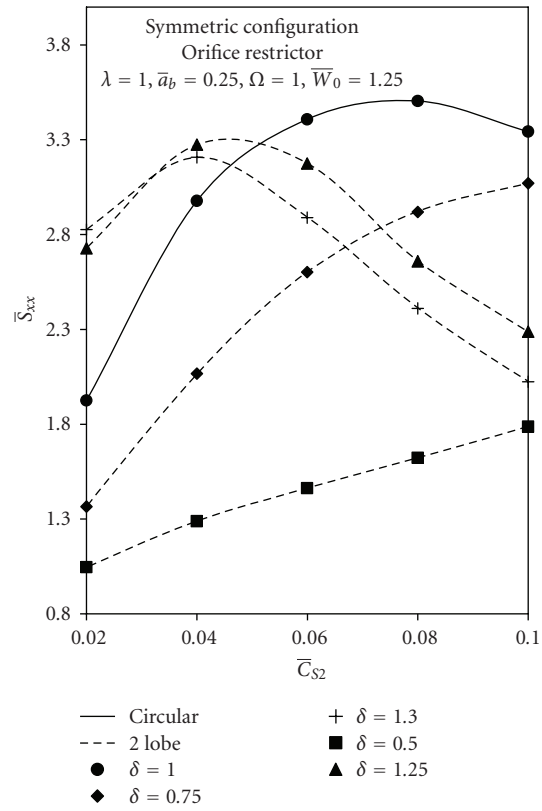

Figure 7: Variation of direct stiffness ($\overline{S}_{xx}$).

two-lobe hole-entry journal bearing by carefully selecting the value of restrictor design parameter ($\overline{C}_{S2}$) and offset factor (δ).

At a constant value of external load ($\overline{W}_0$), the bearing flow ($\overline{Q}$) in Figure 6 is found to be lower for the case of two-lobe hole-entry hybrid journal bearing with offset factor (δ) greater than one compared to bearing flow in circular hole-entry hybrid journal bearing. But the bearing flow is higher for the case of two-lobe hole-entry journal bearing with offset factor less than one. This change in bearing flow may be accounted for the change in profile of the bearing due to change in offset factor (δ). The decrease in the flow rate in case of two-lobe hole-entry hybrid journal bearing with offset greater than one minimizes the pumping power.

The effects of offset factor (δ) on the value of direct stiffness coefficients ($\overline{S}_{xx}, \overline{S}_{zz}$) have been presented in Figures 7 and 8. From Figure 7, it may be observed that there exists a particular value of restrictor design parameter ($\overline{C}_{S2}$) at which the value of direct stiffness coefficient ($\overline{S}_{xx}$) is the maximum for a particular case of offset factor (δ). As seen from Figure 7, at a value of restrictor design parameter ($\overline{C}_{S2} = .04$), the two-lobe hole-entry hybrid journal bearing with an offset factor $\delta = 1.25$ has the highest value of direct stiffness coefficient ($\overline{S}_{xx}$) and at a value of restrictor design parameter ($\overline{C}_{S2} = .08$), the hole-entry hybrid journal bearing with an offset factor $\delta = 1.0$ has the highest value of direct stiffness coefficient ($\overline{S}_{xx}$). The results from Figure 7

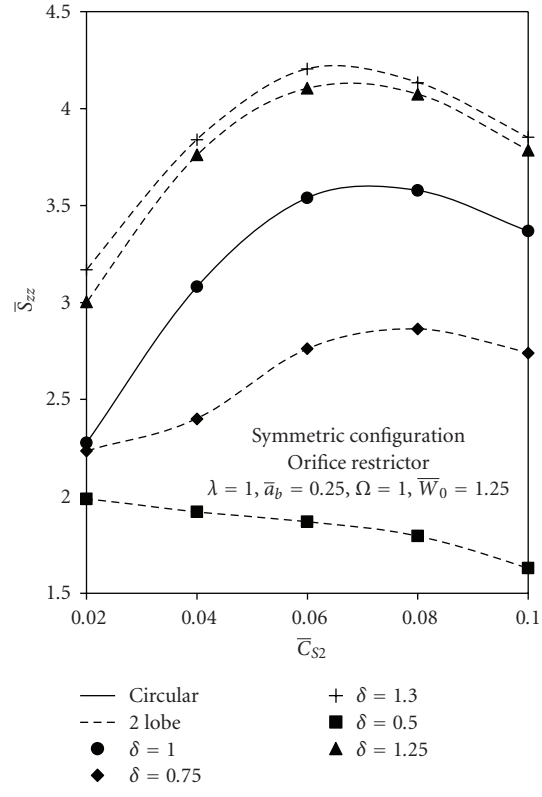

Figure 8: Variation of direct stiffness ($\overline{S}_{zz}$).

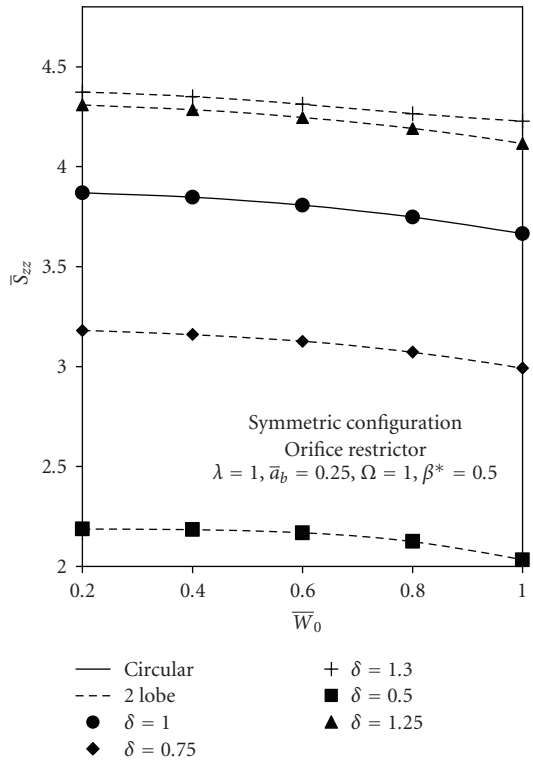

Figure 9: Variation of direct stiffness ($\overline{S}_{zz}$).

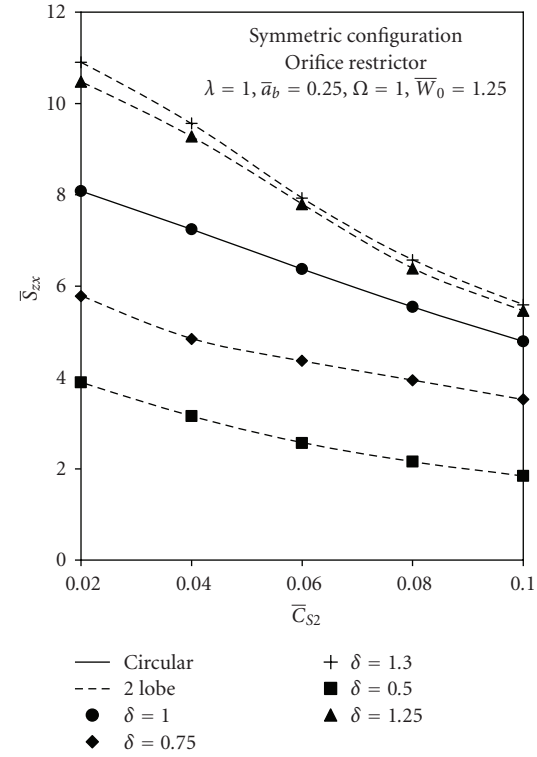

Figure 10: Variation of cross coupled stiffness ($\overline{S}_{zx}$).

indicate that the restrictor design parameter ($\overline{C}_{S2}$) becomes an important parameter when the designer aims to maximize the value of ($\overline{S}_{xx}$) at constant external load ($\overline{W}_0$). Figure 8 shows, at a constant external load $\overline{W}_0$, fluid film stiffness coefficients ($\overline{S}_{zz}$) which in general show an initial increasing trend and then decrease with an increase in restrictor design parameter ($\overline{C}_{S2}$) except for the case of offset factor $\delta = 0.5$. The two-lobe hole-entry hybrid journal bearing indicates a higher value of direct fluid-film stiffness coefficients ($\overline{S}_{zz}$) compared with circular hole-entry hybrid journal bearing for a value of offset factor (δ) greater than one for a chosen load.

Figure 9 shows the effect of direct fluid-film stiffness coefficients ($\overline{S}_{zz}$) with an increase in offset factor (δ). The value of direct fluid-film stiffness coefficient ($\overline{S}_{zz}$) gets decreased with an increase in the value of external load ($\overline{W}_0$) for all the cases of offset factor (δ). Further, it may be observed that the value of direct fluid-film stiffness coefficient ($\overline{S}_{zz}$) is maximum in case of two-lobe hole entry hybrid journal bearing with an offset factor $\delta = 1.3$.

Figure 10 shows the effect of cross coupled fluid-film stiffness coefficients ($\overline{S}_{zx}$) with an increase in offset factor (δ). It can be observed from the figure that the values of $\overline{S}_{zx}$ in case of two-lobe hole-entry journal bearing follow the similar trend for the different values of offset factor (δ). The two-lobe hole-entry hybrid journal bearing with offset factor of 0.5 has the least value of $\overline{S}_{zx}$.

The variation of direct damping coefficients ($\overline{C}_{xx}, \overline{C}_{zz}$) with offset factor ($\delta$) is shown in Figures 11 and 12. At

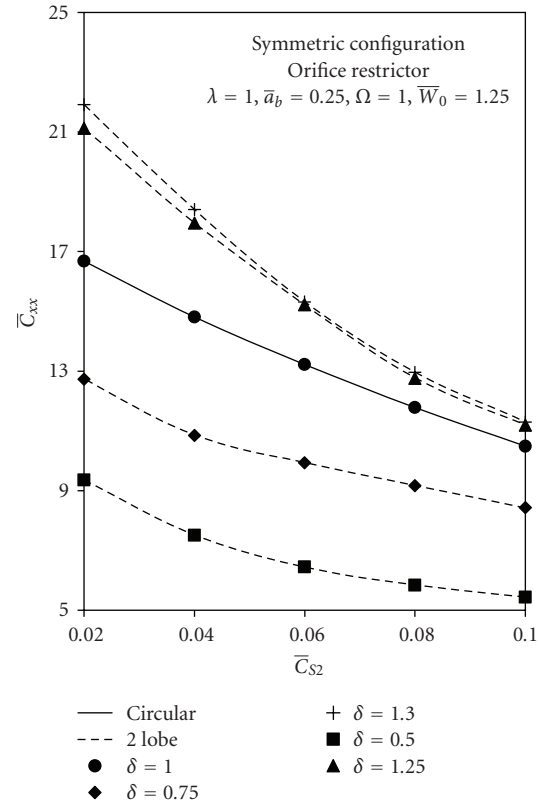

Figure 11: Variation of direct damping ($\overline{C}_{xx}$).

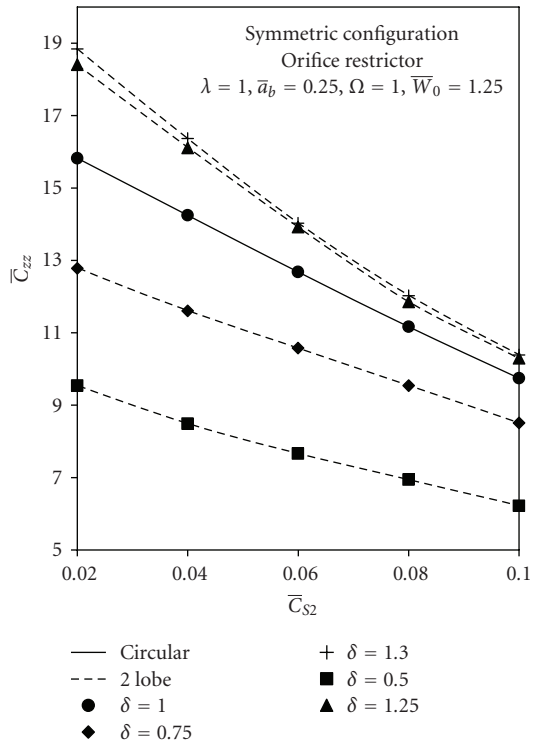

Figure 12: Variation of direct damping ($\overline{C}_{zz}$).

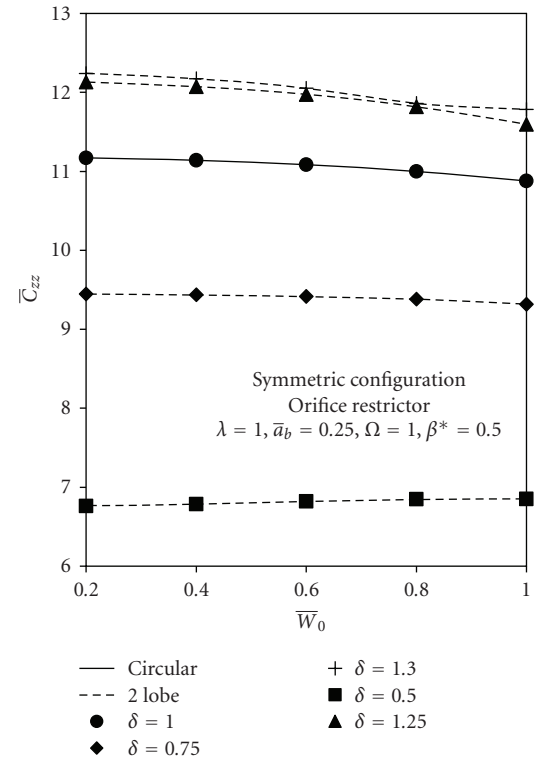

Figure 13: Variation of direct damping ($\overline{C}_{zz}$).

constant load ($\overline{W}_0$), damping coefficients ($\overline{C}_{xx}, \overline{C}_{zz}$) are increased with an increase of offset factor (δ). It is observed from Figures 11 and 12 that the two-lobe hole-entry hybrid journal bearing with offset factor (δ) greater than one exhibits higher value of direct damping coefficients ($\overline{C}_{xx}, \overline{C}_{zz}$) compared to that of circular hole-entry hybrid journal bearing.

Figure 13 shows the variation of direct fluid-film coefficient ($\overline{C}_{zz}$) against restrictor design parameter ($\overline{C}_{S2}$). The value of direct fluid-film damping coefficient ($\overline{C}_{zz}$) gets increased with an increase in offset factor (δ) for the chosen value of external load ($\overline{W}_0$). Further, it may be observed that the value of direct fluid-film damping coefficient ($\overline{C}_{zz}$) decreases with an increase in the value of restrictor design parameter ($\overline{C}_{S2}$) for all the cases of offset factor (δ) except for the case of offset factor $\delta = 0.5$. For the case of offset factor $\delta = 0.5$, the value of direct fluid-film damping coefficient ($\overline{C}_{zz}$) nearly remains a constant with an increase in restrictor design parameter ($\overline{C}_{S2}$).

Figure 14 shows variation with stability threshold speed ($\overline{\omega}_{\text{th}}$) against the restrictor design parameter ($\overline{C}_{S2}$). For a chosen value of load at a constant speed, the system is asymptotically stable when the operating speed of the journal (ω_J) is less than stability threshold ($\overline{\omega}_{\text{th}}$), that is, $\omega_J < \omega_{\text{th}}$. From Figure 7, it may be observed that there exists a particular value of restrictor design parameter ($\overline{C}_{S2}$) at which the value of stability threshold speed ($\overline{\omega}_{\text{th}}$) is the maximum for a particular case of offset factor (δ). As seen from the Figure 7, at a value of restrictor design parameter

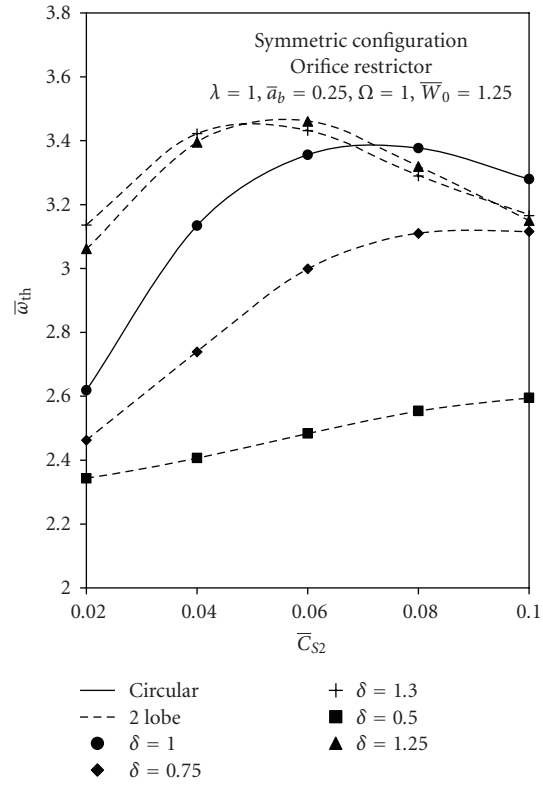

Figure 14: Variation of threshold speed ($\overline{\omega}_{\text{th}}$).

($\overline{C}_{S2} = .06$), the two-lobe hole-entry hybrid journal bearing with an offset factor $\delta = 1.25$ has the highest value of stability threshold speed ($\overline{\omega}_{\text{th}}$) and at a value of restrictor design parameter ($\overline{C}_{S2} = .08$), the hole-entry hybrid journal bearing with an offset factor $\delta = 1.0$ has the highest value of stability threshold speed ($\overline{\omega}_{\text{th}}$). The results from Figure 7 indicate that the restrictor design parameter ($\overline{C}_{S2}$) becomes an important parameter when the designer aims to maximize the value of ($\overline{\omega}_{\text{th}}$) at constant external load ($\overline{W}_0$).

10. CONCLUSIONS

On the basis of the theoretical results presented in the paper, the following conclusions have been drawn.

(1) Two-lobe hole-entry hybrid journal bearing with an offset factor (δ) greater than one requires a reduced quantity of lubricant as compared to circular hybrid hole-entry journal bearing, hence reduced pumping power is needed.

(2) A two-lobe hole-entry hybrid journal bearing system with an offset factor (δ) greater than one provides a larger value of stiffness ($\overline{S}_{zz}$) and damping ($\overline{C}_{xx}$) coefficients. These values are found to be of the order of 15.9% and 36.2%, respectively more vis-a-vis a circular hole-entry journal bearing system for the same value of external load ($\overline{W}_0$) and for the same bearing geometric parameters.

(3) A two-lobe hole-entry journal bearing system with offset factor (δ) greater than one provides enhanced value of stability threshold speed margin of the order of 14.4% to that of circular hole-entry hybrid journal bearing system.

NOMENCLATURE

a_b: Bearing land width, mm
c: Radial clearance, mm
$C_1 = c$, C_2: Clearance due to circumscribed, inscribed circle on the bearing, mm
C_{ij}: Damping coefficients ($i, j = x, z$), N.sec.mm^{-1}
d_0: Orifice diameter, mm
e: Journal eccentricity, mm
h, L: Fluid-film thickness, bearing length mm
t: Time, second
F: Fluid film reaction ($\partial h/\partial t \neq 0$), N
F_0: Fluid film reaction ($\partial h/\partial t = 0$), N
g: Acceleration due to gravity, m.sec^{-2}
R_J, R_b: Radius of journal and bearing, respectively, mm
R_L: Radius of lobe, mm
p, p^*: Pressure, concentric design pressure N.mm^{-2}
Q: Bearing flow, mm^3.sec^{-1}
S_{ij}: Stiffness coefficients, ($i, j = x, z$), N.mm^{-1}
W_0: External load, N
X, Y, Z: Cartesian coordinates
X_J, Z_J: Coordinates of steady-state equilibrium journal center from geometric center of bearing, coordinates, mm
X_L^i, Z_L^i: Lobe center coordinates of the ith lobe
x, z: Horizontal and vertical co-ordinate measured from steady-state equilibrium position of journal center, mm
μ: Dynamic viscosity of lubricant, N.sec.m^{-2}
μ_r: Dynamic viscosity of lubricant at reference temperature and pressure, N.sec.m^{-2}
ω_J, ω_{th}: Journal rotational speed, threshold speed rad.sec^{-1}
ω_I: $(g/c)^{1/2}$, rad.sec^{-1}
ϕ: Attitude angle, rad
ρ: Density of lubricant, kg.mm^{-3}
ψ_d: Coefficient of discharge for orifice

NONDIMENSIONAL PARAMETERS

$\overline{a}_b = a_b/L$: Land width ratio
$\overline{C}_{ij} = C_{ij}(c^3/\mu R_J^4)$
$\overline{C}_{S2} = 1/12(3\pi d_0^2 \mu_r \psi_d/c^3)(2/\rho p_s)^{1/2}$: Orifice design parameter
$(\overline{F}, \overline{F}_0) = (F, F_0)/p_s R_J^2$
$(\overline{h}) = (h)/c$
$(\overline{p}, \overline{p}_s, \overline{p}_c, \overline{p}_{\max}) = (p, p_s, p_c, p_{\max})/p_s$
$\overline{Q} = Q(\mu/c^3 p_s)$
$\overline{S}_{ij} = S_{ij}(c/p_s R_J^2)$
$\overline{W}_0 = W_0/p_s R_J^2$
$(\overline{X}_J, \overline{x}, \overline{Z}_J, \overline{z}) = (X_J, x, Z_J, z)/c$
$(\overline{X}_L^i, \overline{Z}_L^i) = (X_L^i, Z_L^i)/c$
$(\alpha, \beta) = (X, Y)/R_J$: Circumferential axial coordinates
β^* = Concentric design pressure ratio, p^*/p_s
$\varepsilon = e/c$: Eccentricity ratio
$\lambda = L/D$: Aspect ratio
$\Omega = \omega_J(\mu R_J^2/c^2 p_s)$: Speed parameter
$\overline{\omega}_{\text{th}} = \omega_{\text{th}}/\omega_I$
$\overline{t} = t(c^2 p_s/\mu R_J^2)$
$\delta = C_1/C_2$: Offset factor
O_J: Journal center
O_{Li}: Lobe center

MATRICES

$[\overline{F}]$: Fluidity matrix
$\{\overline{p}\}$: Nodal pressure vector
$\{\overline{Q}\}$: Nodal flow vector
$\{\overline{R}_H\}$: Vector due to hydrodynamic terms
$\{\overline{R}_{Xj}\}$, $\{\overline{R}_{Zj}\}$: Right-hand side vectors due to journal center velocities

SUBSCRIPTS AND SUPERSCRIPTS

0: Steady-state solution
J: Journal
R: Restrictor
s: Supply
$-$: Corresponding nondimensional parameter
l: Lobe
i: Lobe number

REFERENCES

[1] O. Pinkus, "Analysis of elliptical bearing," *Transactions of the ASME*, vol. 78, pp. 965–973, 1956.

[2] M. Malik, "A comparative study of some two-lobed journal bearing configurations," *Tribology Transactions*, vol. 26, no. 1, pp. 118–124, 1983.

[3] P. K. Goenka and J. F. Booker, "Effect of surface ellipticity on dynamically loaded cylindrical bearing," *Transactions of the ASME, Journal of Lubrication Technology*, vol. 105, pp. 1–12, 1983.

[4] Y.-M. Yan, Q.-H. Yan, and Q. An, "An numerical study on the influences of preload factor on the properties of three-lobe journal bearing," *Journal of East China University of Science and Technology*, vol. 32, no. 5, pp. 612–616, 2006.

[5] R. Pai and B. C. Majumdar, "Stability of submerged four-lobe oil journal bearings under dynamic load," *Wear*, vol. 154, no. 1, pp. 95–108, 1992.

[6] M. K. Ghosh and A. Nagraj, "Rotordynamic characteristics of a multilobe hybrid journal bearing in turbulent lubrication," *Proceedings of the Institution of Mechanical Engineers, Part J: Journal of Engineering Tribology*, vol. 218, no. 1, pp. 61–67, 2004.

[7] M. K. Ghosh and M. R. Satish, "Rotordynamic characteristics of multilobe hybrid bearings with short sills—part I," *Tribology International*, vol. 36, no. 8, pp. 625–632, 2003.

[8] M. K. Ghosh and M. R. Satish, "Stability of multilobe hybrid bearing with short sills—part II," *Tribology International*, vol. 36, no. 8, pp. 633–636, 2003.

[9] D. Khosal and W. B. Rowe., "Fluid film journal bearings operating in a hybrid mode—part 2: experimental investigations," *Transactions of the ASME, Journal of Lubrication Technology*, vol. 103, no. 4, pp. 566–573, 1981.

[10] W. B. Rowe, S. X. Xu, F. S. Chong, and W. Weston, "Hybrid journal bearings with particular reference to hole-entry configurations," *Tribology International*, vol. 15, no. 6, pp. 339–348, 1982.

[11] S. Yoshimoto, W. B. Rowe, and D. Ives, "A theoretical investigation of the effect of inlet pocket size on the performance of hole-entry hybrid journal bearings employing capillary restrictors," *Wear*, vol. 127, no. 3, pp. 307–318, 1988.

[12] W. B. Rowe, D. Koshal, and K. J. Stout, "Slot-entry bearings for hybrid hydrodynamic and hydrostatic operation," *Journal of Mechanical Engineering Science*, vol. 18, no. 2, pp. 73–78, 1976.

[13] L. Guo and J. Zhu, "Analysis of circular slot entry hybrid bearing—part I," *Journal of Hunan University Natural Sciences*, vol. 23, no. 3, p. 103, 1996.

[14] J. C. T. Su and K. N. Lie, "Rotation effects on hybrid hydrostatic/hydrodynamic journal bearings," *Industrial Lubrication and Tribology*, vol. 53, no. 6, pp. 261–267, 2001.

[15] H. C. Garg, H. B. Sharda, and V. J. Kumar, "On the design and development of hybrid journal bearings: a review," *Tribotest*, vol. 12, no. 1, pp. 1–19, 2006.

[16] S. C. Sharma, R. Sinhasna, and S. C. Jain, "An elastohydrostatic study of hole-entry hybrid flexible journal bearings with capillary restrictors," *Tribology International*, vol. 26, no. 2, pp. 93–107, 1993.

[17] S. C. Sharma, S. C. Jain, and N. M. M. Reddy, "A study of non-recessed hybrid flexible journal bearing with different restrictors," *Tribology Transactions*, vol. 44, no. 2, pp. 310–317, 2001.

[18] K. H. Huebner, *The Finite Element Method for Engineers*, A Wiley-Interscience Publication, John Wiley & Sons, New York, NY, USA, 1975.

[19] J. W. Lund and K. K. Thomsen, "A calculation method and data for the dynamic coefficients of oil lubricated journal bearings," in *Topics In Fluid Film Bearing and Rotor Bearing System Design and Optimization*, pp. 1–28, ASME, New York, NY, USA, 1978.